BIOCHEMISTRY
including biophysical chemistry & molecular biology

Article

pubs.acs.org/biochemistry

Functional Replacement of Two Highly Conserved Tetraloops in the Bacterial Ribosome

Bhubanananda Sahu, Prashant K. Khade, and Simpson Joseph*

Department of Chemistry and Biochemistry, University of California at San Diego, 9500 Gilman Drive, La Jolla, California 92093-0314, United States

ABSTRACT: Ribosomes are RNA−protein complexes responsible for protein synthesis. A dominant structural motif in the rRNAs is an RNA helix capped with a four-nucleotide loop, called a tetraloop. The sequence of the tetraloop is invariant at some positions in the rRNAs but is highly variable at other positions. The biological reason for the conservation of the tetraloop sequence at specific positions in the rRNAs is not clear. In the 16S rRNA, the GAAA tetraloop in helix 8 and the UACG tetraloop in helix 14 are highly conserved and located near the binding site for EF-Tu and EF-G. To investigate whether the structural stability of the tetraloop or the precise sequence of the tetraloop is important for function, we separately changed the GAAA tetraloop in helix 8 to a UACG tetraloop and the UACG tetraloop in helix 14 to a GAAA tetraloop. The effects of the tetraloop replacements on protein synthesis were analyzed in vivo and in vitro. Replacement of the tetraloops in helices 8 and 14 did not significantly affect the growth rate of the *Escherichia coli* (Δ7rrn) strain. However, the mutant ribosomes showed a slightly reduced rate of protein synthesis in vitro. In addition, we observed a 2-fold increase in the error rate of translation with the mutant ribosomes, which is consistent with an earlier report. Our results suggest that the tetraloops in helices 8 and 14 are highly conserved mainly for their structural stability and the precise sequences of these tetraloops are not critical for protein synthesis.

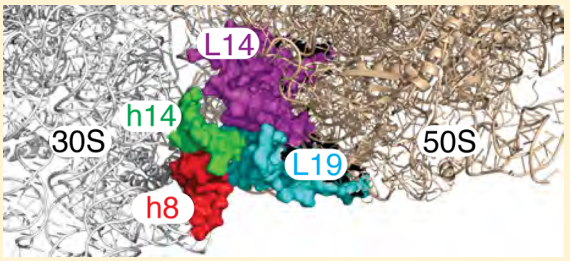

Ribosomes are megadalton-sized complexes consisting of both RNA and protein. In bacteria, the 30S ribosomal subunit is composed of a 16S rRNA and ∼21 proteins and the 50S ribosomal subunit is composed of 23S rRNA, 5S rRNA, and ∼30 proteins. The three-dimensional structure of the 30S and 50S subunits, to a large extent, is established by the folded structure of the rRNAs.[1] A common structural motif in the rRNAs is the tetraloop.[2] A tetraloop is a small loop composed of four residues connecting the two antiparallel chains of an RNA helix (Figure 1). Tetraloops have exceptionally high thermodynamic stability and function as nucleation sites for folding large RNA molecules.[3,4] On the basis of their consensus sequence, there are four major types of tetraloops: GNRA, UNCG, CUYG, and GANC (where N is any of the four nucleotides, R is a purine, and Y is a pyrimidine).[2,3,5,6]

Interestingly, nearly 90% of all the tetraloops in the 16S rRNA are GNRA or UNCG.[2] The overall fold adopted by the GNRA and UNCG tetraloops is similar[7,8] (Figure 1A−D). In both GNRA and UNCG, the first and fourth bases form hydrogen bonds, the nonconserved second base is flipped out of the loop, and the phosphate backbone between the second and the third nucleotides is extended for closing the loop. Nevertheless, the GNRA and UNCG tetraloops differ significantly in their local structure and dynamics.[3] In the GNRA tetraloop, the base G is in a 5′ stack and the last two bases are in a 3′ stack. In contrast, in the UNCG tetraloop, the first base U and the third base C are in a 5′ stack and the fourth base G is in a 3′ stack. The second and third nucleotides in the GNRA loop have highly flexible sugar conformation alternating equally between the 2′-endo and 3′-endo conformers, whereas in the UNCG loop, the second and third nucleotides remain essentially in the 2′-endo sugar conformation. These differences make the UNCG loop thermodynamically more stable but less dynamic than the GNRA loop. By being more dynamic, the GNRA loop often can form long-range tertiary interactions, unlike the UNCG loop.[3,9−11] Thus, the greater flexibility of the GNRA loop permits it to play a more specialized role in the folding and function of large RNAs.

Despite these differences in the structure and dynamics of the GNRA and UNCG tetraloops, a previous study showed that a GNRA loop found in the signal recognition particle RNA could be functionally interchanged with an UNCG loop, suggesting that the tetraloops sometimes act as a unit.[12] In contrast, studies with group I self-splicing introns showed that a GNRA loop cannot be functionally interchanged with an UNCG loop.[9,13] Here, the GNRA loop is important for function because it forms a tertiary interaction that is required for stabilizing the folded state of the self-splicing intron. Therefore, in some cases, the precise sequence of the tetraloop is more important for function than a thermodynamically stable structure. In the ribosome, there are several highly conserved tetraloops at particular positions in the rRNAs.[2,14] The reason for the conservation of a GNRA versus an UNCG tetraloop at a particular position in the rRNAs is not clear. They may be

Received: July 11, 2012
Revised: August 30, 2012
Published: August 31, 2012

dx.doi.org/10.1021/bi300930r | *Biochemistry* 2012, 51, 7618−7626

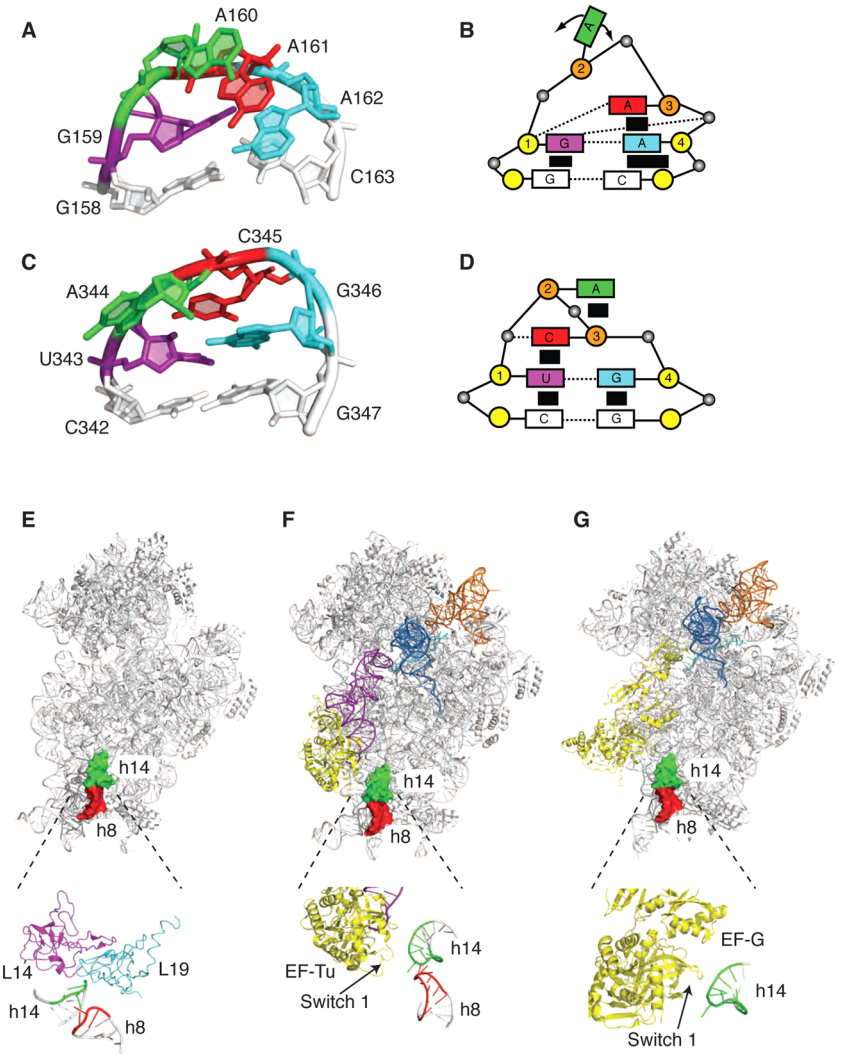

Figure 1. Structural features of the two studied tetraloops and their location in the ribosome. (A) Tertiary structure of the GAAA tetraloop in helix 8 (Protein Data Bank entry 2AVY).[15] The bases that form the tetraloop are G159 (purple), A160 (green), A161 (red), and A162 (cyan). The G-C base pair of the RNA stem is colored gray. (B) Schematic representation of the GAAA tetraloop. Shown are the bases (rectangles, which are color-coded as described above), phosphates (black spheres), and sugars (yellow circles for the 3′-endo sugar conformation and orange circles for the 2′-endo sugar conformation). The hydrogen bonds are indicated by the dotted lines, and the stacking interactions are indicated by the black rectangles. Base G1 is in a 5′ stack, and A3 and A4 are in a 3′ stack. (C) Tertiary structure of the UACG tetraloop in helix 14 (Protein Data Bank entry 2AVY).[15] The bases that form the tetraloop are U343 (purple), A344 (green), C345 (red), and G346 (cyan). The C-G base pair of the RNA stem is colored gray. (D) Schematic representation of the UACG tetraloop. The coloring scheme and labels are as described above for the GAAA tetraloop. Bases U1 and C3 are in a 5′ stack, and base G4 is in a 3′ stack. (E) Structure of the 30S subunit showing the location of helices 8 and 14 of the 16S rRNA (Protein Data Bank entry 2AVY).[15] Shown are the 30S subunit (gray), the GAAA tetraloop in h8 (red), and the UACG tetraloop in h14 (green). The interaction of helix 14 with the 50S subunit ribosomal proteins L14 (magenta) and L19 (cyan) to form the bridge B8 is shown below. (F) Interaction of EF-Tu with helices 8 and 14 of the 16S rRNA (Protein Data Bank entry 3FIH).[20] Shown are the 30S subunit (gray), the GAAA tetraloop in h8 (red), the UACG tetraloop in h14 (green), EF-Tu (yellow), A-tRNA (purple), P-tRNA (sky blue), and E-tRNA (orange). A close-up of the interaction between the switch 1 loop in EF-Tu and the junction of helices 8 and 14 is shown below. (G) Interaction of EF-G with helices 8 and 14 of the 16S rRNA in the post-translocation state (Protein Data Bank entry 2WRI).[46] Shown are the 30S subunit (gray), the GAAA tetraloop in h8 (red), the UACG tetraloop in h14 (green), EF-G (yellow), P-tRNA (sky blue), and E-tRNA (orange). A close-up of the interaction between the switch 1 loop in EF-G and helix 14 is shown below (Protein Data Bank entry 2OM7).[22]

conserved purely for their structural stability, the ability to form tertiary interactions, or some functional role during protein synthesis such as binding translation factors.

To determine whether the thermodynamic stability and the ability to form sequence specific tertiary interactions account for the conservation of a tetraloop sequence at a particular position in the rRNAs, we decided to analyze two highly conserved tetraloops in 16S rRNA. We selected the GAAA tetraloop in helix 8 and the UACG tetraloop in helix 14 of 16S rRNA, which are located in the shoulder domain of the 30S subunit (Figure 1E). Interestingly, the GAAA tetraloop in helix 8 has the precise geometry for making an A-minor tertiary interaction with helix 14 except it appears to be out of contact range in the crystal structures.[15] Noller has made the intriguing proposal that some of the GNRA loops that are out of contact range of their receptor helix may form tertiary interactions during defined steps of translation to stabilize distinct conformational states of the ribosome.[16] The UACG tetraloop in helix 14 contacts the large ribosomal subunit proteins L14 and L19 to form intersubunit bridge B8 (Figure 1E).[15,17−19]

dx.doi.org/10.1021/bi300930r | *Biochemistry* 2012, 51, 7618−7626

Cryo-EM structures showed that the switch I domain of elongation factor Tu (EF-Tu) contacts the junction of helices 8 and 14 (Figure 1F).[20,21] In addition, switch I of elongation factor G (EF-G) interacts with helix 14[22,23] (Figure 1G).

Consistent with the structural data, mutations in helices 8 and 14 have been shown to increase the error rate of translation, indicating a functional role for these tetraloops during tRNA selection.[24] However, mutations can change the structure and thermodynamic stability of the tetraloop, leading to more pronounced functional defects. We, instead, chose to replace as a unit one type of tetraloop with another type of tetraloop to maintain the overall structure and stability of the hairpin but with a different sequence. We analyzed the effect of these tetraloop replacements using biochemical assays. Our results show that the helix 8 and helix 14 tetraloop replacements do not significantly affect the function of the ribosome, suggesting that the precise sequences of these two tetraloops are not essential for translation.

EXPERIMENTAL PROCEDURES

Site-Directed Mutagenesis of 16S rRNA. Site-directed mutagenesis was performed with a QuickChange polymerase chain reaction mutagenesis kit (Stratagene). Plasmid pLK35-16S-MS2 was used as the template to replace ^{158}g(GAAA)c^{163} with c(UACG)g in helix 8 and ^{343}UACG^{346} with GAAA in helix 14 of 16S rRNA.[25,26] All clones were verified by automated DNA sequencing of the entire 16S rRNA operon.

Plasmid-Replacement Strategy. Plasmid replacement was performed as described previously.[27,28] Briefly, *Escherichia coli* strain SQZ10 (Δ7rrn) containing plasmid pHK-rrnC$^+$sacB (kanamycin resistant) was transformed with pLK35-16S-MS2 containing the desired mutations. The transformants were grown overnight in LB medium (10 g of tryptone, 5 g of yeast extract, and 10 g of NaCl per liter of medium) with 100 μg/mL ampicillin at 37 °C while being shaken. The cultures were diluted and plated on 2YT agar plates with 8% sucrose and 100 μg/mL ampicillin. The colonies on the plates were screened for sensitivity to kanamycin by replica plating. Plasmid replacement was confirmed by isolating plasmids and automated DNA sequencing. Cell stocks were prepared in 15% glycerol and stored at −80 °C.

Growth Curve. Growth of plasmid-replaced *E. coli* strain SQZ10 (Δ7rrn) expressing the wild-type or mutant 16S rRNA occurred in 200 μL of LB medium in the presence of 100 μg/mL ampicillin at 37 °C with continuous shaking in a plate reader (Genios, Tecan).[26] Each culture was inoculated with the same number of cells from overnight starter cultures. The absorbance at 600 nm was automatically measured at 10 min intervals by the plate reader. The data were fit to an exponential growth curve equation ($Y = Ae^{bx}$), and the doubling time was calculated as $\ln(2)/b$ using Prism (GraphPad Prism, San Diego, CA).

Ribosome Profile. Ribosome profiles of *E. coli* strain SQZ10 (Δ7rrn) expressing the wild-type or mutant 16S rRNA were determined essentially as described previously.[26]

In Vitro Translation of the Reporter Protein. The activity of the purified ribosome was analyzed by in vitro translation of the reporter protein *Renilla* luciferase as described previously.[25,26] Briefly, activated ribosomes were added to the S-100 in vitro translation mix and transferred to a 96-well plate. The 96-well plate was incubated at 37 °C in a plate reader (Genios, Tecan), and the synthesis of the luciferase enzyme was monitored in real time by measuring the luminescence every 2 min. Duplicates of the samples were used for each experiment, and the assays were repeated at least twice.

Peptidyl Transferase Assay by Quench-Flow Methods. Peptidyl transferase reactions were performed in HiFi buffer [50 mM Tris-HCl (pH 7.5), 70 mM NH_4Cl, 30 mM KCl, 3.5 mM $MgCl_2$, 8 mM putrescine, 0.5 mM spermine, and 2 mM DTT] as described previously.[29] Initiation complexes were prepared in HiFi buffer (with 7 mM Mg^{2+}) by incubation of the activated 70S ribosome (2.5 μM) with mRNA (5 μM) at 37 °C for 10 min. The [^{35}S]fMet-tRNA^{fMet} charging mixture was prepared in HiFi buffer (3.75 μM tRNA^{fMet}, 3 mM ATP, 0.25 μM [^{35}S]-L-methionine, 3.75 μM L-methionine, 0.4 mM N^{10}-formyltetrahydrofolic acid, 10 μg of formyl transferase, and 10 μg of MetRS incubated at 37 °C for 20 min) added directly to the ribosome−mRNA complex, and the incubation was continued at 37 °C for 10 min. Unbound [^{35}S]fMet-tRNA^{fMet} was removed by ultrafiltration using Microcon Centrifugal Filter Devices (Amicon; 100000 molecular weight cutoff) and by washing six times with 400 μL of HiFi buffer (7 mM Mg^{2+}). The initiation complexes were recovered after washing, and the concentration of Mg^{2+} was adjusted to 3.5 mM via addition of HiFi buffer without Mg^{2+}. To prepare the EF-Tu·GTP·Phe-tRNA^{Phe} ternary complex, the EF-Tu·GTP complex was formed via incubation of 1 mM GTP, 3 mM phosphoenolpyruvate, 0.25 μg/μL pyruvate kinase, and 1.5 μM EF-Tu at 37 °C for 20 min in HiFi buffer. Phe-tRNA^{Phe} (0.5 μM) was then added, and the incubation was continued for an additional 20 min. To determine the rate of the peptidyl transferase reaction, 15 μL of the 70S initiation complex was rapidly mixed with 15 μL of the ternary complex and the reaction quenched with 1 M KOH in a quench-flow instrument (μQFM-400, BioLogic). The dipeptide was resolved by electrophoresis on cellulose TLC plates and quantified using a phosphorimager (Bio-Rad).

Estimation of Missense Error and Nonsense Error by an in Vivo Reporter Assay. To estimate the frequency of missense errors, the activity of the *Renilla* luciferase (RL) mutant (Glu144Asp) relative to that of wild-type RL (control) was determined using *E. coli* strain SQZ10 (Δ7rrn) expressing the wild-type or mutant 16S rRNA. The mutation of the catalytic residue Glu144 (codon GAA) to Asp (codon GAT) decreases the reporter activity to 5%.[30] Any miscoding at codon GAT will be reflected as increased reporter activity. A similar approach was used to estimate the frequency of UGA read-through (nonsense errors). To estimate the nonsense error, the activity of the *Renilla* luciferase mutant (Leu156Stop) relative to that of wild-type RL (control) was determined for *E. coli* strain SQZ10 (Δ7rrn) expressing the wild-type or mutant 16S rRNA. The stop codon is in the middle of the catalytic tried of *Renilla* luciferase D120, E144, and H285,[30] and it abolishes luciferase activity completely. Read-through of the stop codon will be reflected as increased reporter activity.

In Vitro Fidelity Experiment. The in vitro fidelity experiments were performed as described previously.[29]

Translocation Experiment. Pretranslocation complexes were made, and translocation was monitored by the toeprinting assay as described previously.[31] Rapid kinetic experiments were performed essentially as described previously.[26,32]

RESULTS

Replacing the Tetraloops in Helices 8 and 14 Does Not Affect the Growth Rate. To study the significance of the conservation of the GAAA tetraloop in helix 8 and the UACG tetraloop in helix 14, we separately replaced these tetraloop

sequences by site-directed mutagenesis in plasmid pLK35-MS2-16S.[33] The GAAA tetraloop in helix 8 was replaced with the UACG tetraloop to create the h8 mutant (h8). Replacement of the GNRA tetraloop with the UNCG tetraloop is expected to disfavor the formation of the A-minor tertiary interaction with helix 14. The UACG tetraloop in helix 14 was replaced with a GAAA tetraloop to create the h14 mutant (h14). Replacement of the UNCG tetraloop with the GNRA tetraloop is expected to disrupt any sequence specific interactions between helix 14 and EF-Tu and EF-G. In addition, bridge B8 may also be disrupted, resulting in weakened association of the 30S subunit with the 50S subunit.

We used *E. coli* strain SQZ10 (Δ7rrn) to analyze the effect of the tetraloop replacements on cell growth. *E. coli* strain SQZ10 (Δ7rrn) lacks the seven rRNA operons in its genome and survives by having the rRNA genes expressed from a plasmid.[27,28] The h8 and h14 mutant plasmids were transformed into *E. coli* strain SQZ10 (Δ7rrn) and selected using the appropriate antibiotic. Our plasmid replacement studies showed that *E. coli* strain SQZ10 could grow normally with either the h8 or the h14 mutant plasmids exclusively expressing the rRNA genes (data not shown). Growth rate studies in liquid cultures at 37 and 42 °C further confirmed that the growth rates of the h8 and h14 mutants are similar to that of the wild type (doubling times at 37 °C of 60 ± 1, 62 ± 1, and 62 ± 3 min for WT, h8, and h14, respectively). Thus, the replacement of h8 or h14 with a different type of tetraloop does not appreciably affect the growth rate.

Replacing the h14 Tetraloop Causes a Modest Defect in Subunit Association. We analyzed the ribosome profile of h8 and h14 mutant cells to identify defects in 30S subunit assembly and in their association with the 50S subunit to form 70S ribosome. The ribosome profile showed that the h8 mutant has no defects in 30S assembly and in subunit association (Figure 2). In contrast, the h14 mutant showed a small shoulder to the left of the 70S peak, suggesting that the mutant 30S subunit does not bind tightly to the 50S subunit and dissociate during the centrifugation (Figure 2C). Thus, the h14 mutant likely has subtle defects in subunit association. It is well-known that increasing the Mg^{2+} ion concentration from 10 to 20 mM can improve subunit association. Therefore, we repeated the ribosome analysis in the presence of 20 mM Mg^{2+} ion. As expected, the h14 mutant 30S subunit showed normal subunit association at the higher Mg^{2+} ion concentration (Figure 2E).

Inhibition of in Vitro Translation by the Tetraloop Replacements. We analyzed the activity of the mutant ribosomes in protein synthesis using an in vitro translation assay. The time course of *Renilla* luciferase synthesis by the wild-type and mutant ribosomes was monitored by bioluminescence[25] (Figure 3). The experiment was conducted at several ribosome concentrations. Our results showed that the wild-type ribosomes efficiently synthesize luciferase at a final concentration of 0.1 μM (Figure 3A). In contrast, 0.2 μM h8 mutant ribosomes and 0.4 μM h14 mutant ribosomes are required to achieve a similar rate of luciferase synthesis (Figure 3B,C). Thus, the in vitro translation assay indicates that the mutant ribosomes are slightly defective in in vitro protein synthesis.

Tetraloop Replacements Do Not Affect the Peptidyl Transferase Reaction. Structural data showed that the switch 1 loop of EF-Tu interacts with the junction of helix 8 and helix 14.[20,21] Therefore, to determine whether the replacement of the

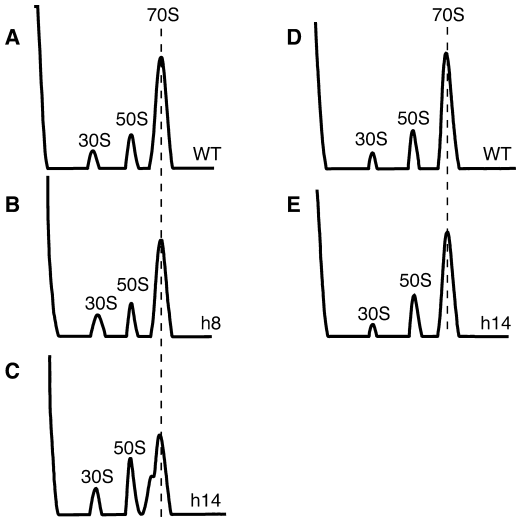

Figure 2. Ribosome profile of cells expressing mutant 16S rRNAs: (A) wild type, (B) h8 mutant, (C) h14 mutant, (D) wild type (with 20 mM $MgCl_2$), and (E) h14 mutant (with 20 mM $MgCl_2$). The wild-type and mutant 16S rRNAs were expressed in *E. coli* strain SQZ10 (Δ7rnr). Experiments A–C were performed in buffer containing 10 mM $MgCl_2$. Experiments D and E were performed in buffer containing 20 mM $MgCl_2$. Labels: 30S, small ribosomal subunit; 50S, large ribosomal subunit; 70S, ribosome. The dotted line indicates the position of the 70S ribosome in the sucrose gradient.

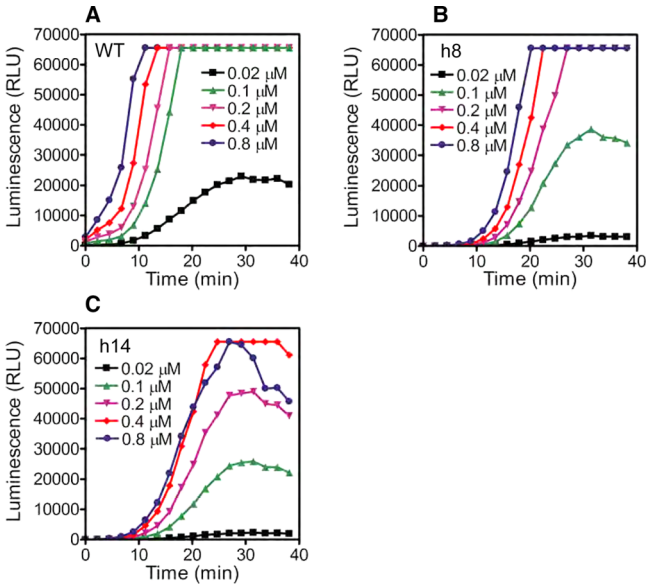

Figure 3. In vitro protein synthesis by mutant ribosomes. Representative time courses showing the synthesis of the luciferase enzyme at the indicated concentrations of the wild-type and mutant ribosomes: (A) wild-type ribosome, (B) h8 mutant ribosome, and (C) h14 mutant ribosome. The in vitro protein synthesis was conducted at 6 mM $MgCl_2$. The maximal signal that we can observe with this instrument is ≈65000 relative luminescence units (RLU) because of detector saturation.

h8 and h14 tetraloops affected the rate of peptide bond formation, we conducted pre-steady state kinetic experiments. The ribosome with [^{35}S]fMet-tRNA^{fMet} in the P site and a phenylalanine codon in the A site was rapidly mixed with a nearly saturating concentration of the EF-Tu·GTP·Phe-tRNA^{Phe} ternary complex with a quench-flow instrument.[29]

dx.doi.org/10.1021/bi300930r | *Biochemistry* 2012, 51, 7618–7626

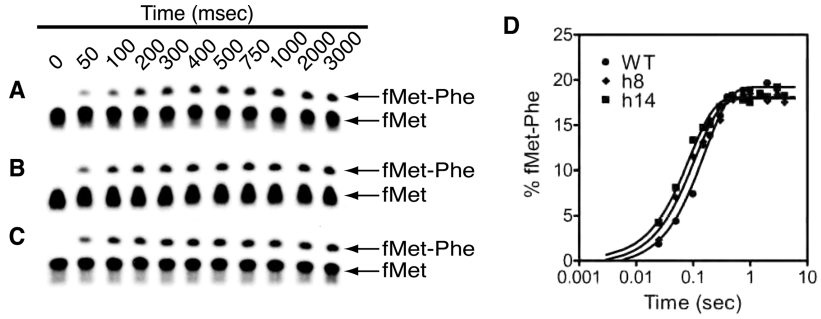

Figure 4. Kinetics of peptide bond formation. Representative electrophoretic TLC plates showing the time course of dipeptide formation by wild-type and mutant ribosomes: (A) wild-type ribosome, (B) h8 mutant ribosome, and (C) h14 mutant ribosome. (D) Graph showing the time course of dipeptide formation by wild-type ribosome (●), h8 mutant ribosome (◆), and h14 mutant ribosome (■). Data were fit to a single-exponential equation to determine the apparent rate of peptide bond formation.

The product of the reaction, [^{35}S]fMet-Phe dipeptide, was analyzed by electrophoretic TLC (eTLC) (Figure 4). The time course of fMet-Phe dipeptide formation was fit to a single-exponential equation to determine the rate of peptide bond formation (6.1 ± 0.3, 8.5 ± 1.2, and 9.9 ± 2.0 s^{-1} for WT, h8, and h14, respectively). The rate of peptide bond formation was similar for wild-type, h8 mutant, and h14 mutant ribosomes, indicating that tRNA selection is not significantly affected by the mutations.

Interchanging the Tetraloops Decreases the Fidelity of Translation. A previous study showed that mutations in h8 and h14 increase the error frequency of protein synthesis by 2–3-fold.[24] Therefore, we determined the in vivo missense error rates of cells expressing the h8 or h14 replacement. The *Renilla* luciferase gene was used as the reporter for determining the fidelity of translation. The catalytic triad of Asp120, Glu144, and His285 in *Renilla* luciferase is essential for the activity of the enzyme.[30] Mutation of these catalytic residues decreases the activity of *Renilla* luciferase to <5%.[30] We measured the missense error rates using a *Renilla* luciferase gene with a point mutation that changes the essential glutamic acid at position 144 to an aspartic acid (codon GAA to GAU). An increase in the rate of misincorporation of glutamic acid at position 144 will increase the amount of active luciferase produced by the cell. Luciferase activity can be detected easily and with high sensitivity by monitoring bioluminescence. We found that both h8 and h14 mutant cells had a missense error rate that was ∼2-fold higher than that of wild-type cells (Figure 5A).

We next determined the rate of nonsense suppression by h8 and h14 mutants. For this, we used a *Renilla* luciferase gene with a point mutation that changes a leucine at position 156 to a stop codon (codon UGG to UGA). Leucine 156 is not essential for the activity of luciferase, and substitution with any other amino acid is tolerated at this position.[30] However, termination of protein synthesis at position 156 will lead to a truncated luciferase enzyme that is inactive. This permitted us to determine the rate of nonsense suppression during protein synthesis. We found that the nonsense suppression rate was increased by 2-fold with the h8 and h14 mutant cells compared to that with the wild-type cells (Figure 5A).

To confirm the increased error rate of protein synthesis by the h8 and h14 mutant ribosomes, we used a simplified in vitro miscoding assay.[29] For the in vitro miscoding assay, we formed a ribosomal complex containing [^{35}S]fMet-tRNA^{fMet} in the P site and a phenylalanine codon (UUU) in the A site. The ribosome complex was mixed with the EF-Tu·GTP·aminoacyl-tRNA ternary complex formed from a mixture of *E. coli* total

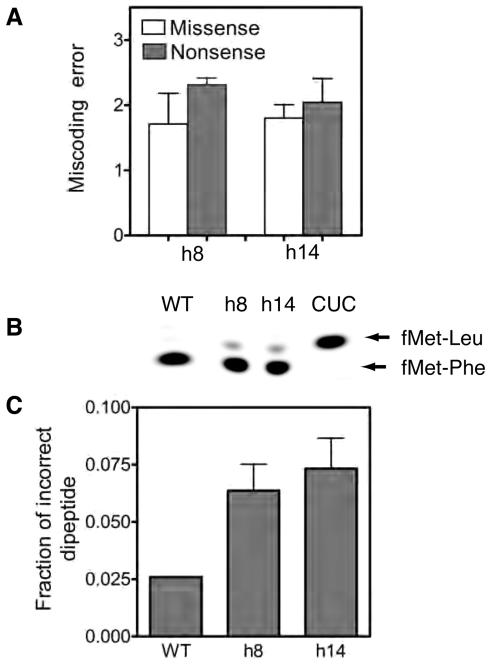

Figure 5. Effects of 16S rRNA mutations on miscoding by the ribosome. (A) Bar graph showing the miscoding error determined using an in vivo reporter assay. Missense and nonsense errors were calculated from *Renilla* luciferase activity in *E. coli* strain SQZ10 (Δ7rnr) expressing wild-type or mutant 16S rRNAs. The error rate of cells expressing wild-type 16S rRNA was normalized to 1.0. Values on the *X*-axis reflect the fold increases in miscoding error by cells expressing h8 and h14 mutant 16S rRNAs compared to cells expressing wild-type 16S rRNA. The data shown are averages ± the standard deviation from three independent experiments. (B) Representative electrophoretic TLC plate showing the products of the in vitro fidelity experiment. Binding of the cognate Phe-tRNA^{Phe} to the ribosomal A site produces the [^{35}S]fMet-Phe dipeptide, whereas binding of the near-cognate Leu-tRNA^{Leu} to the ribosomal A site produces the [^{35}S]fMet-Leu dipeptide. Label CUC shows a control reaction with the wild-type ribosome having a CUC codon in the A site that was performed in parallel to serve as a marker for the [^{35}S]fMet-Leu dipeptide. (C) Bar graph showing the fraction of incorrect [^{35}S]fMet-Leu dipeptide formed by wild-type (WT), h8, and h14 ribosomes.

tRNA. The expected dipeptides are [^{35}S]fMet-Phe for cognate and [^{35}S]fMet-Leu for near-cognate binding of the ternary complex to the ribosome. We analyzed the dipeptides formed by the ribosome by eTLC (Figure 5B). Our results showed that

dx.doi.org/10.1021/bi300930r | *Biochemistry* 2012, 51, 7618–7626

h8 and h14 mutant ribosomes had an error frequency that was 2−3-fold higher than that of the wild-type ribosome and are consistent with the error rates measured in vivo (Figure 5C).

Tetraloop Replacements Do Not Affect Translocation of the mRNA−tRNA Complex. We analyzed whether the tetraloop replacements in h8 and h14 affected EF-G-dependent translocation of the mRNA−tRNA complex by the ribosome. Initially, we used the toeprinting assay to monitor the translocation of the mRNA−tRNA complex by the ribosome.[31,34] Pretranslocation complexes were programmed with a fragment of the T4 gene 32 mRNA and contained $tRNA^{fMet}$ in the P site and $tRNA^{Phe}$ in the A site. The extension of a DNA primer hybridized to the 3′ end of the mRNA by reverse transcriptase resulted in a toeprint band that is characteristic for the pretranslocation complex (Figure 6A). The addition of EF-G and GTP to the pretranslocation complexes resulted in the appearance of a new toeprint band that corresponds to the post-translocation complex. Both h8 and h14 mutants gave extents of translocation similar to that of the wild-type ribosome.

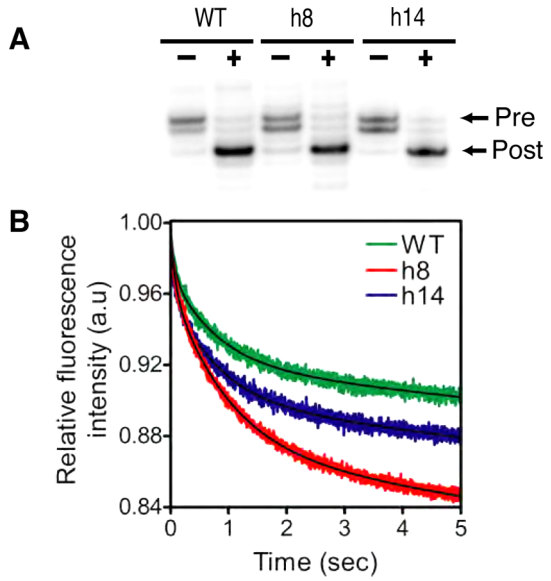

Figure 6. Translocation of the mRNA−tRNA complex. (A) The extent of translocation of the mRNA−tRNA complex was determined using a toeprinting assay. Minus and plus indicate the absence and presence of EF-G, respectively. Toeprinting bands corresponding to the pretranslocation complex (Pre) and the post-translocation complex (Post) are indicated. (B) Pre-steady state kinetic analysis of EF-G-dependent translocation of wild-type and mutant ribosomes. The decrease in fluorescence corresponds to EF-G-dependent translocation of the mRNA−tRNA complex. The data were fit to a double-exponential equation to determine the apparent rate of translocation.

The rate of translocation by the h8 and h14 mutant ribosomes was determined using a fluorescence-based, pre-steady state kinetic assay.[32] The pretranslocation complex contained a short mRNA having a pyrene dye attached to the 3′ terminus, $tRNA^{fMet}$ in the P site, and fMet-Phe-$tRNA^{Phe}$ in the A site. The pretranslocation complex was rapidly mixed with a 10-fold excess of EF-G with a stopped-flow instrument, and the decrease in fluorescence intensity of the pyrene dye because of translocation was recorded (Figure 6B). The change in fluorescence intensity showed two phases with apparent rate constants k_{obs1} and k_{obs2} for the fast and slow phases, respectively. The reason for the two phases is not clear but has been reported previously.[26,35−37] The rate of the rapid phase is consistent with the rate of translocation measured using fluorescently labeled tRNAs.[38] Furthermore, translocation inhibitors such as viomycin and neomycin inhibit the rapid phase.[32,37] The slow phase may be caused by sample heterogeneity or a conformational change in the ribosome that occurs after translocation of the mRNA−tRNA complex. The data were analyzed by fitting the decrease in fluorescence intensity to a double-exponential equation to calculate k_{obs1} and k_{obs2} for the wild-type, h8, and h14 ribosomes (for WT, k_{obs1} = 15.8 ± 0.3 s^{-1} and k_{obs2} = 1.3 ± 0.01 s^{-1}; for h8, k_{obs1} = 11.3 ± 0.3 s^{-1} and k_{obs2} = 1.1 ± 0.1 s^{-1}; for h14, k_{obs1} = 18.7 ± 0.6 s^{-1} and k_{obs2} = 1.2 ± 0.1 s^{-1}). The rates of translocation by the h8 and the h14 mutants were <2-fold different from that of the wild type, suggesting that the mutations do not substantially affect translocation.

DISCUSSION

The ribosome is a precisely assembled molecular machine sculpted out of RNA and protein. The rRNAs not only provide the framework for the overall shape of the ribosome but also are intimately involved in forming the functional centers of the ribosome.[39,40] A dominant secondary structural element of the rRNAs is the hairpin.[2,14,41,42] Approximately 70% of the 16S rRNA folds into stem−loop structures.[2,14] The number and sequence of the nucleotides that form the loop are variable; however, the most common loops in 16S rRNA are tetraloops with the GNRA or UNCG consensus sequence.[2] These tetraloops form compact structures and have very high thermodynamic stability.[3,4,7,8] Despite their similarity in shape and stability, the rRNAs show a strong preference for the GNRA and the UNCG loops at specific positions in the rRNA.[2] The basis for this conservation of the tetraloop sequence at particular positions in the rRNAs is not clear. Woese and co-workers have suggested that the stability of a particular tetraloop sequence itself may be the primary determinant for their conservation at some positions in the rRNAs.[2]

To test whether the primary sequence or the structural stability of the tetraloops is important for ribosome function, we examined two tetraloops in the 16S rRNA that are >99% conserved. We picked the GNRA-type tetraloop in h8 and the UNCG-type tetraloop in h14 because structural studies have suggested that they might be important for translation. Cryo-EM structures showed that the junction between h8 and h14 tetraloops interacts with the switch I region in the GTPase domain of EF-Tu[20,21] (Figure 1F). The interaction of switch I of EF-Tu with the junction of helices h8 and h14 of the 16S rRNA was proposed to open the "hydrophobic gate" in EF-Tu and reorient the catalytic His84 to induce GTP hydrolysis.[20,21] Similarly, the switch I regions of EF-G-GMPPNP (Figure 1G) and eEF2 trapped in the transition state interact with h14 of the 16S rRNA.[22,23] The switch I region of EF4 (LepA) also interacts with h14.[43] However, the interactions of EF-Tu and EF-G with helices 8 and 14 were not observed in recently determined crystal structures.[44−46] It is possible that these crystal structures represent a state that is different from that of the cryo-EM structures.

Another function attributed to helix 14 is the formation of an intersubunit bridge. The UACG tetraloop in helix 14 contacts ribosomal proteins L14 and L19 in the 50S subunit to form intersubunit bridge B8[15,17−19] (Figure 1E). Interestingly, the

dx.doi.org/10.1021/bi300930r | Biochemistry 2012, 51, 7618−7626

30S subunit can undergo a ratchetlike rotation relative to the 50S subunit spontaneously.[47,48] Furthermore, the binding of some translational factors such as EF-G, RF3, and RRF induces the ratchetlike rotation of the ribosome to varying degrees.[49−52] Recent structural data showed that the interactions that h14 makes with L14 and L19 change when the 30S subunit undergoes a ratchetlike rotation relative to the 50S subunit. For example, in the classical state, bridge B8 is formed by nucleotide C345 in the h14 tetraloop interacting with Ser116 and Ala118 in L14 and Arg39 and Arg41 in L19.[50] In the 70S·RF3 complex, bridge B8 rearranges and nucleotide C345 in h14 tetraloop interacts only with Ser35 and Lys36 in L19.[50] In addition, nucleotide G347 in h14 makes new contacts with Leu118 and Ala119 in L14.[50] The phosphate nonbridging oxygens atoms of C345 and G347 mainly mediate these new bridge interactions in the rotated state.[50] Nevertheless, the integrity of bridge B8 may depend on the local structure and thermodynamic stability of the h14 tetraloop.

Genetic and biochemical studies also indicate a functional role for helices 8 and 14. Previously, the A161G mutation in the h8 tetraloop was isolated in a dominant negative screen, and this mutation reduced translation activity in vivo by ≈25%.[53] Another genetic screen isolated several mutations in h8 and h14 tetraloops that increase the rate of misreading of sense and stop codons.[24] These mutations in h8 and h14 also reduced translation activity in vivo by 2−4-fold. Interestingly, they showed that shortening helix 14 by 2 bp decreased the rate of translation by 5-fold, whereas lengthening helix 14 by 2 bp abolished translation in vivo.[24] Lengthening helix 14 is probably not tolerated because it disrupts bridge B8 and prevents subunit association. Furthermore, 2 or 3 bp deletions in helix 8 or a 2 bp deletion in helix 14 increases the missense error rate by 10-fold compared to that of the wild-type ribosome.[24] The increased missense error rate is caused by an increase in the rate of GTP hydrolysis by the near-cognate EF-Tu ternary complex binding to the h8 and h14 mutant ribosomes compared to the wild-type ribosome.[24] Thus, the biochemical data suggest that the h8−h14 junction negatively regulates GTP hydrolysis on EF-Tu.[24] Mutations in helices 8 and 14 may weaken bridge B8 and lower the energetic cost for the conformational changes that induce GTP hydrolysis on EF-Tu. This will lead to an increase in the error rate because even the near-cognate EF-Tu ternary complex can trigger GTP hydrolysis and be accepted by the ribosome.[24]

We find that the complete replacement of the conserved tetraloops in h8 and h14 with a tetraloop having a different sequence is better tolerated by the cells compared to the single-base mutations, deletions, and insertions discussed above. We did not observe any defects in the growth rates of the *E. coli* strain (Δ7rrn) expressing the h8 and h14 mutant plasmids. This is consistent with the idea that the GNRA and UNCG tetraloops have a similar fold and comparable thermodynamic stability and can be functionally interchanged if the precise sequence is not critical for function.[3,12] In contrast, mutations, deletions, and insertions show an increased number of defects in translation because they may be more disruptive to the local or global structure of the ribosome. However, we note that the growth rate of the *E. coli* strain (Δ7rrn) is slower than those of wild-type *E. coli* strains and minor defects in protein synthesis may not significantly affect the growth rate of the *E. coli* strain (Δ7rrn).

We observed a slight defect in subunit association with the h14 mutant at 10 mM Mg^{2+} ion, which is consistent with h14 forming intersubunit bridge B8. However, the subunit association defect was overcome at 20 mM Mg^{2+} ion. It is possible that Mg^{2+}, polyamines, and the high concentrations of 30S and 50S subunits present in vivo may stabilize subunit association even with a GNRA loop in helix 14. This is consistent with our observation that increasing the concentration of the h8 and h14 mutant 30S subunits could increase the rate of in vitro translation. Interestingly, the rate of in vitro translation is slower with the h8 and h14 mutant ribosomes. Because these experiments were performed at 6 mM $MgCl_2$, it is possible that during the initiation step of translation the rate of association of the 50S subunit to the mutant 30S subunits is slower than to the wild-type 30S subunit, explaining the slow rate of in vitro translation. More studies are necessary to understand whether the h8 and h14 tetraloop replacements inhibit translation initiation.

Our studies showed that the h8 and h14 mutants have rates of peptide bond formation and translocation that are similar to those of the wild-type ribosome. Thus, the precise sequence of h8 and h14 is not essential for these steps in the elongation cycle of protein synthesis. Nevertheless, the h8 and h14 mutants showed an ∼2-fold increased error rate of translation. The increased rate of miscoding, however, is much lower than the 5−10-fold increase in the rate of miscoding reported previously with single-base substitutions and the deletion mutants.[24] Therefore, in helices 8 and 14, changing the conserved sequence of the tetraloop as a unit with a different tetraloop sequence is better tolerated by the ribosome. This may be a useful strategy for determining whether the conservation of a tetraloop sequence at a particular position in the rRNAs is essential for protein synthesis. Finally, our results suggest that the conservation of a tetraloop sequence at a particular position in the rRNAs may come from evolutionary pressures to maintain the stability of the tetraloop structure itself instead of a defined function during protein synthesis.

AUTHOR INFORMATION

Corresponding Author

*Address: 4102 Urey Hall, Department of Chemistry and Biochemistry, University of California at San Diego, 9500 Gilman Dr., La Jolla, CA 92093-0314. Phone: (858) 822-2957. E-mail: sjoseph@ucsd.edu.

Funding

This work was supported by National Institutes of Health Grant GM065265 to S.J.

Notes

The authors declare no competing financial interest.

ACKNOWLEDGMENTS

We thank Kurt Fredrick, Ulrich Muller, and Gourisankar Ghosh for comments on the manuscript.

ABBREVIATIONS

rRNA, ribosomal RNA; mRNA, messenger RNA; tRNA, translation RNA; EF, elongation factor.

REFERENCES

(1) Ramakrishnan, V., and Moore, P. B. (2001) Atomic structures at last: The ribosome in 2000. *Curr. Opin. Struct. Biol. 11*, 144−154.

(2) Woese, C. R., Winker, S., and Gutell, R. R. (1990) Architecture of ribosomal RNA: Constraints on the sequence of "tetra-loops". *Proc. Natl. Acad. Sci. U.S.A. 87*, 8467−8471.

(3) Varani, G. (1995) Exceptionally stable nucleic acid hairpins. *Annu. Rev. Biophys. Biomol. Struct. 24*, 379−404.
(4) Uhlenbeck, O. C. (1990) Tetraloops and RNA folding. *Nature 346*, 613−614.
(5) Butcher, S. E., and Pyle, A. M. (2011) The molecular interactions that stabilize RNA tertiary structure: RNA motifs, patterns, and networks. *Acc. Chem. Res. 44*, 1302−1311.
(6) Keating, K. S., Toor, N., and Pyle, A. M. (2008) The GANC tetraloop: A novel motif in the group IIC intron structure. *J. Mol. Biol. 383*, 475−481.
(7) Cheong, C., Varani, G., and Tinoco, I., Jr. (1990) Solution structure of an unusually stable RNA hairpin, 5′GGAC(UUCG)-GUCC. *Nature 346*, 680−682.
(8) Heus, H. A., and Pardi, A. (1991) Structural features that give rise to the unusual stability of RNA hairpins containing GNRA loops. *Science 253*, 191−194.
(9) Jaeger, L., Michel, F., and Westhof, E. (1994) Involvement of a GNRA tetraloop in long-range RNA tertiary interactions. *J. Mol. Biol. 236*, 1271−1276.
(10) Costa, M., and Michel, F. (1995) Frequent use of the same tertiary motif by self-folding RNAs. *EMBO J. 14*, 1276−1285.
(11) Pley, H. W., Flaherty, K. M., and McKay, D. B. (1994) Model for an RNA tertiary interaction from the structure of an intermolecular complex between a GAAA tetraloop and an RNA helix. *Nature 372*, 111−113.
(12) Selinger, D., Liao, X., and Wise, J. A. (1993) Functional interchangeability of the structurally similar tetranucleotide loops GAAA and UUCG in fission yeast signal recognition particle RNA. *Proc. Natl. Acad. Sci. U.S.A. 90*, 5409−5413.
(13) Murphy, F. L., and Cech, T. R. (1994) GAAA tetraloop and conserved bulge stabilize tertiary structure of a group I intron domain. *J. Mol. Biol. 236*, 49−63.
(14) Cannone, J. J., Subramanian, S., Schnare, M. N., Collett, J. R., D'Souza, L. M., Du, Y., Feng, B., Lin, N., Madabusi, L. V., Müller, K. M., Pande, N., Shang, Z., Yu, N., and Gutell, R. R. (2002) The Comparative RNA Web (CRW) Site: An online database of comparative sequence and structure information for ribosomal, intron, and other RNAs. *BMC Bioinf. 3*, 2.
(15) Schuwirth, B. S., Borovinskaya, M. A., Hau, C. W., Zhang, W., Vila-Sanjurjo, A., Holton, J. M., and Cate, J. H. (2005) Structures of the bacterial ribosome at 3.5 Å resolution. *Science 310*, 827−834.
(16) Noller, H. F. (2005) RNA structure: Reading the ribosome. *Science 309*, 1508−1514.
(17) Yusupov, M. M., Yusupova, G. Z., Baucom, A., Lieberman, K., Earnest, T. N., Cate, J. H., and Noller, H. F. (2001) Crystal structure of the ribosome at 5.5 Å resolution. *Science 292*, 883−896.
(18) Korostelev, A., Trakhanov, S., Laurberg, M., and Noller, H. F. (2006) Crystal structure of a 70S ribosome-tRNA complex reveals functional interactions and rearrangements. *Cell 126*, 1065−1077.
(19) Selmer, M., Dunham, C. M., Murphy, F. V. t., Weixlbaumer, A., Petry, S., Kelley, A. C., Weir, J. R., and Ramakrishnan, V. (2006) Structure of the 70S ribosome complexed with mRNA and tRNA. *Science 313*, 1935−1942.
(20) Villa, E., Sengupta, J., Trabuco, L. G., LeBarron, J., Baxter, W. T., Shaikh, T. R., Grassucci, R. A., Nissen, P., Ehrenberg, M., Schulten, K., and Frank, J. (2009) Ribosome-induced changes in elongation factor Tu conformation control GTP hydrolysis. *Proc. Natl. Acad. Sci. U.S.A. 106*, 1063−1068.
(21) Schuette, J. C., Murphy, F. V. t., Kelley, A. C., Weir, J. R., Giesebrecht, J., Connell, S. R., Loerke, J., Mielke, T., Zhang, W., Penczek, P. A., Ramakrishnan, V., and Spahn, C. M. (2009) GTPase activation of elongation factor EF-Tu by the ribosome during decoding. *EMBO J. 28*, 755−765.
(22) Connell, S. R., Takemoto, C., Wilson, D. N., Wang, H., Murayama, K., Terada, T., Shirouzu, M., Rost, M., Schuler, M., Giesebrecht, J., Dabrowski, M., Mielke, T., Fucini, P., Yokoyama, S., and Spahn, C. M. (2007) Structural basis for interaction of the ribosome with the switch regions of GTP-bound elongation factors. *Mol. Cell 25*, 751−764.
(23) Sengupta, J., Nilsson, J., Gursky, R., Kjeldgaard, M., Nissen, P., and Frank, J. (2008) Visualization of the eEF2-80S ribosome transition-state complex by cryo-electron microscopy. *J. Mol. Biol. 382*, 179−187.
(24) McClory, S. P., Leisring, J. M., Qin, D., and Fredrick, K. (2010) Missense suppressor mutations in 16S rRNA reveal the importance of helices h8 and h14 in aminoacyl-tRNA selection. *RNA 16*, 1925−1934.
(25) Garcia-Ortega, L., Stephen, J., and Joseph, S. (2008) Precise alignment of peptidyl tRNA by the decoding center is essential for EF-G-dependent translocation. *Mol. Cell 32*, 292−299.
(26) Shi, X., Chiu, K., Ghosh, S., and Joseph, S. (2009) Bases in 16S rRNA important for subunit association, tRNA binding, and translocation. *Biochemistry 48*, 6772−6782.
(27) Asai, T., Condon, C., Voulgaris, J., Zaporojets, D., Shen, B., Al-Omar, M., Squires, C., and Squires, C. L. (1999) Construction and initial characterization of *Escherichia coli* strains with few or no intact chromosomal rRNA operons. *J. Bacteriol. 181*, 3803−3809.
(28) Asai, T., Zaporojets, D., Squires, C., and Squires, C. L. (1999) An *Escherichia coli* strain with all chromosomal rRNA operons inactivated: Complete exchange of rRNA genes between bacteria. *Proc. Natl. Acad. Sci. U.S.A. 96*, 1971−1976.
(29) Hetrick, B., Khade, P. K., Lee, K., Stephen, J., Thomas, A., and Joseph, S. (2010) Polyamines accelerate codon recognition by transfer RNAs on the ribosome. *Biochemistry 49*, 7179−7189.
(30) Woo, J., Howell, M. H., and von Arnim, A. G. (2008) Structure-function studies on the active site of the coelenterazine-dependent luciferase from Renilla. *Protein Sci. 17*, 725−735.
(31) Joseph, S., and Noller, H. F. (1998) EF-G-catalyzed translocation of anticodon stem-loop analogs of transfer RNA in the ribosome. *EMBO J. 17*, 3478−3483.
(32) Studer, S. M., Feinberg, J. S., and Joseph, S. (2003) Rapid Kinetic Analysis of EF-G-dependent mRNA Translocation in the Ribosome. *J. Mol. Biol. 327*, 369−381.
(33) Lancaster, L., and Noller, H. F. (2005) Involvement of 16S rRNA nucleotides G1338 and A1339 in discrimination of initiator tRNA. *Mol. Cell 20*, 623−632.
(34) Hartz, D., McPheeters, D. S., Traut, R., and Gold, L. (1988) Extension inhibition analysis of translation initiation complexes. *Methods Enzymol. 164*, 419−425.
(35) Walker, S. E., Shoji, S., Pan, D., Cooperman, B. S., and Fredrick, K. (2008) Role of hybrid tRNA-binding states in ribosomal translocation. *Proc. Natl. Acad. Sci. U.S.A. 105*, 9192−9197.
(36) Ermolenko, D. N., and Noller, H. F. (2011) mRNA translocation occurs during the second step of ribosomal intersubunit rotation. *Nat. Struct. Mol. Biol. 18*, 457−462.
(37) Khade, P. K., and Joseph, S. (2011) Messenger RNA interactions in the decoding center control the rate of translocation. *Nat. Struct. Mol. Biol. 18*, 1300−1302.
(38) Savelsbergh, A., Katunin, V. I., Mohr, D., Peske, F., Rodnina, M. V., and Wintermeyer, W. (2003) An elongation factor G-induced ribosome rearrangement precedes tRNA-mRNA translocation. *Mol. Cell 11*, 1517−1523.
(39) Korostelev, A., Ermolenko, D. N., and Noller, H. F. (2008) Structural dynamics of the ribosome. *Curr. Opin. Chem. Biol. 12*, 674−683.
(40) Schmeing, T. M., and Ramakrishnan, V. (2009) What recent ribosome structures have revealed about the mechanism of translation. *Nature 461*, 1234−1242.
(41) Noller, H. F., Kop, J., Wheaton, V., Brosius, J., Gutell, R. R., Kopylov, A. M., Dohme, F., Herr, W., Stahl, D. A., Gupta, R., and Waese, C. R. (1981) Secondary structure model for 23S ribosomal RNA. *Nucleic Acids Res. 9*, 6167−6189.
(42) Noller, H. F., and Woese, C. R. (1981) Secondary structure of 16S ribosomal RNA. *Science 212*, 403−411.
(43) Connell, S. R., Topf, M., Qin, Y., Wilson, D. N., Mielke, T., Fucini, P., Nierhaus, K. H., and Spahn, C. M. (2008) A new tRNA intermediate revealed on the ribosome during EF4-mediated back-translocation. *Nat. Struct. Mol. Biol. 15*, 910−915.

(44) Schmeing, T. M., Voorhees, R. M., Kelley, A. C., Gao, Y. G., Murphy, F. V. t., Weir, J. R., and Ramakrishnan, V. (2009) The crystal structure of the ribosome bound to EF-Tu and aminoacyl-tRNA. *Science 326*, 688−694.
(45) Voorhees, R. M., Schmeing, T. M., Kelley, A. C., and Ramakrishnan, V. (2010) The mechanism for activation of GTP hydrolysis on the ribosome. *Science 330*, 835−838.
(46) Gao, Y. G., Selmer, M., Dunham, C. M., Weixlbaumer, A., Kelley, A. C., and Ramakrishnan, V. (2009) The structure of the ribosome with elongation factor G trapped in the posttranslocational state. *Science 326*, 694−699.
(47) Cornish, P. V., Ermolenko, D. N., Noller, H. F., and Ha, T. (2008) Spontaneous intersubunit rotation in single ribosomes. *Mol. Cell 30*, 578−588.
(48) Munro, J. B., Altman, R. B., Tung, C. S., Cate, J. H., Sanbonmatsu, K. Y., and Blanchard, S. C. (2010) Spontaneous formation of the unlocked state of the ribosome is a multistep process. *Proc. Natl. Acad. Sci. U.S.A. 107*, 709−714.
(49) Frank, J., and Agrawal, R. K. (2000) A ratchet-like inter-subunit reorganization of the ribosome during translocation. *Nature 406*, 318−322.
(50) Zhou, J., Lancaster, L., Trakhanov, S., and Noller, H. F. (2012) Crystal structure of release factor RF3 trapped in the GTP state on a rotated conformation of the ribosome. *RNA 18*, 230−240.
(51) Jin, H., Kelley, A. C., and Ramakrishnan, V. (2011) Crystal structure of the hybrid state of ribosome in complex with the guanosine triphosphatase release factor 3. *Proc. Natl. Acad. Sci. U.S.A. 108*, 15798−15803.
(52) Dunkle, J. A., Wang, L., Feldman, M. B., Pulk, A., Chen, V. B., Kapral, G. J., Noeske, J., Richardson, J. S., Blanchard, S. C., and Cate, J. H. (2011) Structures of the bacterial ribosome in classical and hybrid states of tRNA binding. *Science 332*, 981−984.
(53) Yassin, A., Fredrick, K., and Mankin, A. S. (2005) Deleterious mutations in small subunit ribosomal RNA identify functional sites and potential targets for antibiotics. *Proc. Natl. Acad. Sci. U.S.A. 102*, 16620−16625.